Electronic Supplementary Material (ESI) for Polymer Chemistry.
This journal is © The Royal Society of Chemistry 2020

Supporting information

Photo-induced Copper Mediated Copolymerization of Activated-ester Methacrylate Polymers and Their Use as Reactive Precursors to Prepare Multi-dentate Ligands for the Water Transfer of Inorganic Nanoparticles

Binh T. Mai,[$]* Markus J. Barthel,[$] Aidin Lak,[$] Tommaso Avellini,[$] Ana Maria Panaite,[$] Emille M. Rodrigues, Luca Goldoni[$], and Teresa Pellegrino[$]*

[$] Istituto Italiano di Tecnologia (IIT), via Morego 30, 16163 Genoa, Italy

*Email: thanh-binh.mai@iit.it, teresa.pellegrino@iit.it;

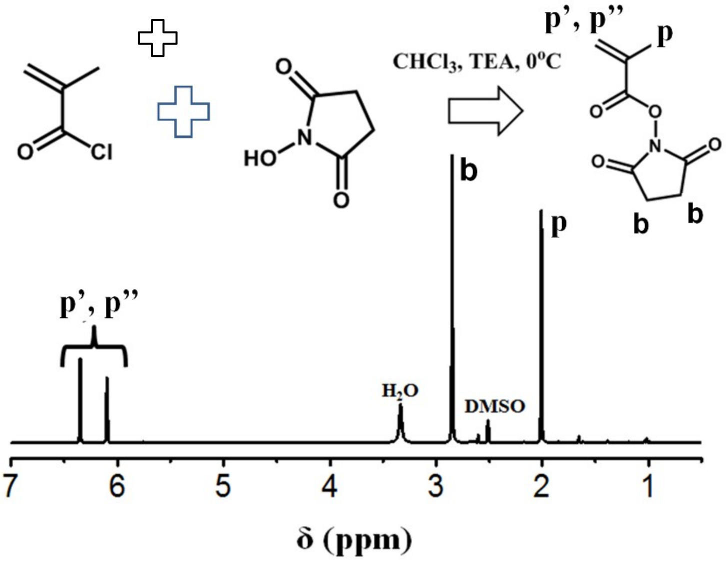

Figure S1. Schematic representation for the synthesis of N-succinimidyl methacrylate, one of the monomers used for the synthesis of P(NSMA-*co*-PEGMA), and its ^{1}H NMR spectrum (recorded in DMSO-d_6 at 25°C, on a Bruker 400 MHz BBI spectrometer).

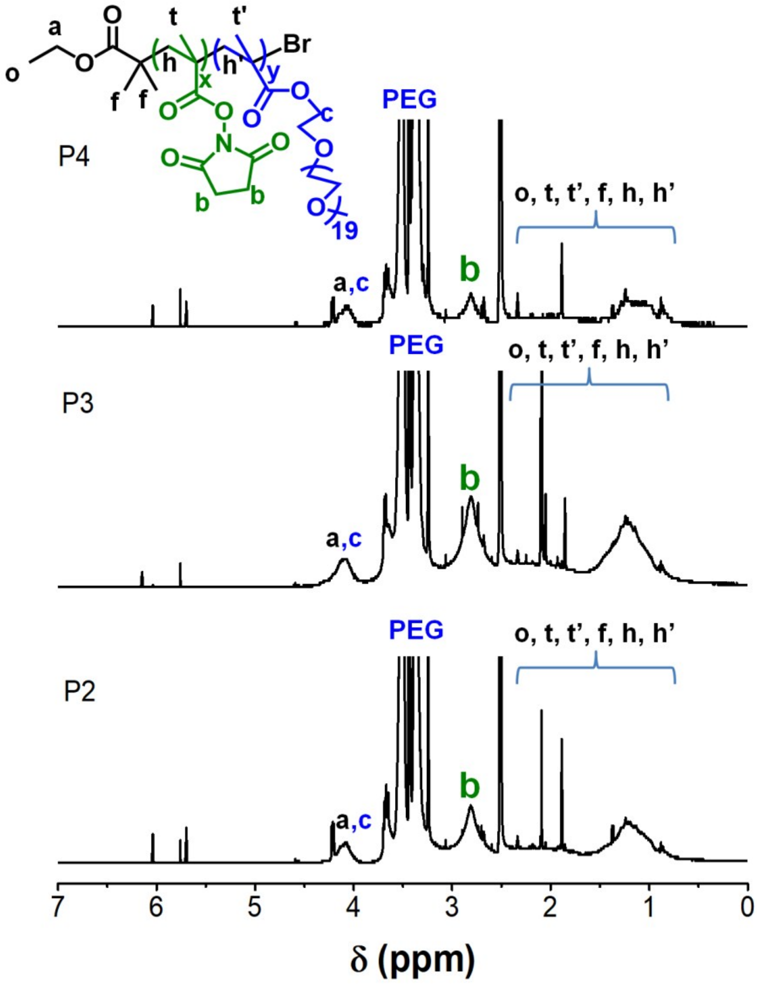

Figure S2. ^{1}H NMR spectra of P2, P3 and P4 (recorded in DMSO-d_6 at 25 °C, on a Bruker 400 MHz BBI spectrometer).

Table S1. The data related the kinetic study of P1

Time (h)	PEGMA conversion (%)	NSMA conversion (%)	NSMA in copolymer (%)	M_n theory (g.mol^{-1})	M_n SEC (g.mol^{-1})	Đ
2	6.5	14.3	68.6	2200	23200	1.18
3	19.0	26.5	58.1	5800	24800	1.21
4	27.4	43.9	61.6	8500	25300	1.25
5	35.7	54.0	59.6	11000	25800	1.29
7	46.4	68.3	59.5	14300	26400	1.31
18	83.3	97.9	54.0	24300	23200	1.28

$$M_n theory = \frac{[NSMA]_0}{[EtBriBu]_0} \times Conversion_{NSMA} \times 183 + \frac{[OEGMEMA]_0}{[EtBriBu]_0} \times Conversion_{OEGMEMA} \times 950 + 195 \quad \text{(E1)}$$

Where $[NSMA]_0$, $[PEGMA]_0$ and $[EtBriBu]_0$ are the initial concentration of NSMA, PEGMA and EtBriBu, respectively. Here we assumed a quantitative initiation efficiency of the initiator to calculate the theoretical molar masses of resulting polymers.

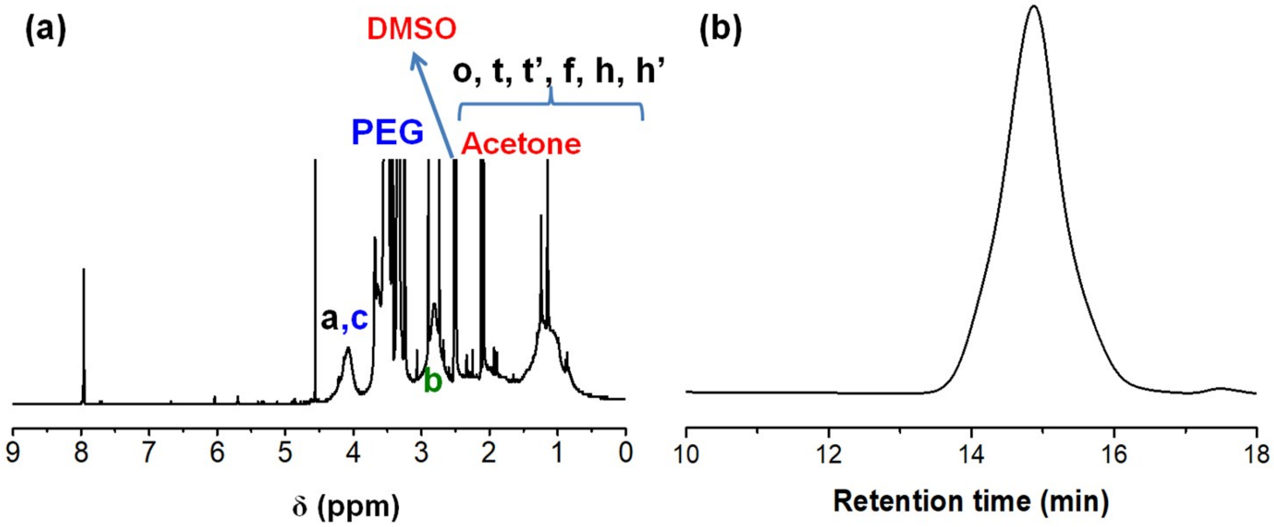

Figure S3. (a) The ^{1}H NMR spectrum (recorded in DMSO-d_6, on a Bruker 400 MHz BBI spectrometer and (b) SEC trace of the copolymer obtained after 18 h of irradiation (eluent: THF).

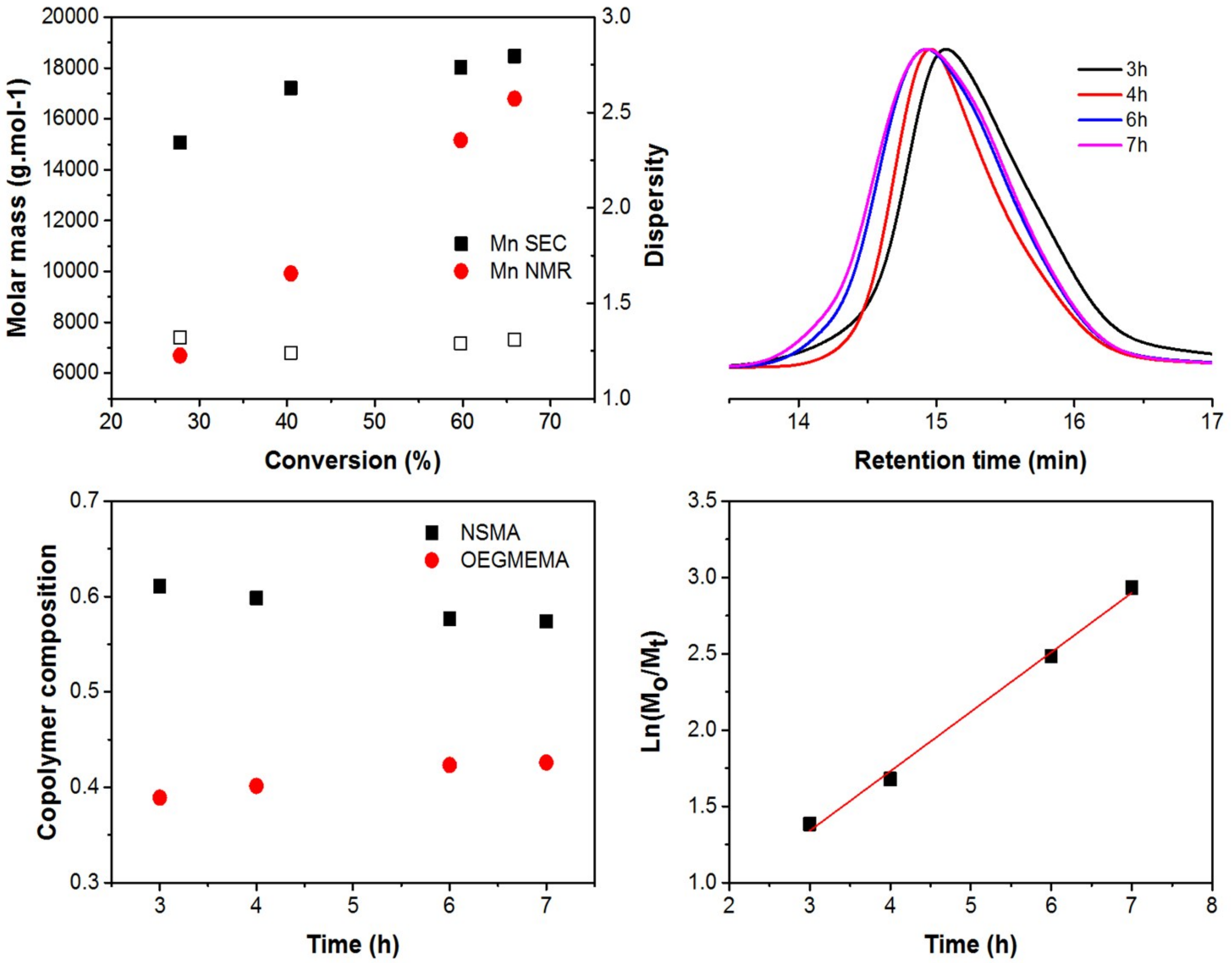

Figure S4. Kinetics for the PI-CMRP of sample adapting a similar condition used for P1 using PEGMA$_{500}$ instead of PEGMA$_{950}$; (a) evolution of molar mass (M$_n$) and dispersity (Đ) with total monomer conversion; (b) SEC traces (eluent: THF) showing the evolution of molar mass with polymerization time; (c) The composition of copolymers at various time and (d) semi-logarithmic plot of total monomer conversion versus time.

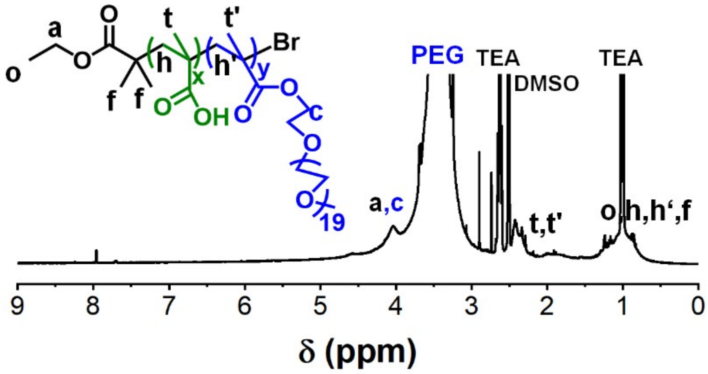

Figure S5. ^{1}H NMR spectra of P1 upon the simple hydrolysis in the identical condition used for the synthesis of P(PEGMA$_{950}$-*co*-AEPMA) (recorded in DMSO-d_6 at 25 ^{o}C, on a Bruker 400 MHz BBI spectrometer).

Table S2. The recovery yield of iron upon water transfer

IONCs edge (nm)	Volume of chloroform (mL)	Concentration of iron in original $CHCl_3$ solution* ($g.L^{-1}$)	Volume of saline (mL)	Concentration of iron in saline solution* ($g.L^{-1}$)
12	1.0	2.05	1.0	1.85
18	1.0	1.95	1.0	1.72
23	1.0	2.15	1.0	1.66
28	1.0	1.80	1.0	1.53

* Determined by Induced Coupling Plasma-Atomic Emission Spectroscopy (ICP-AES)

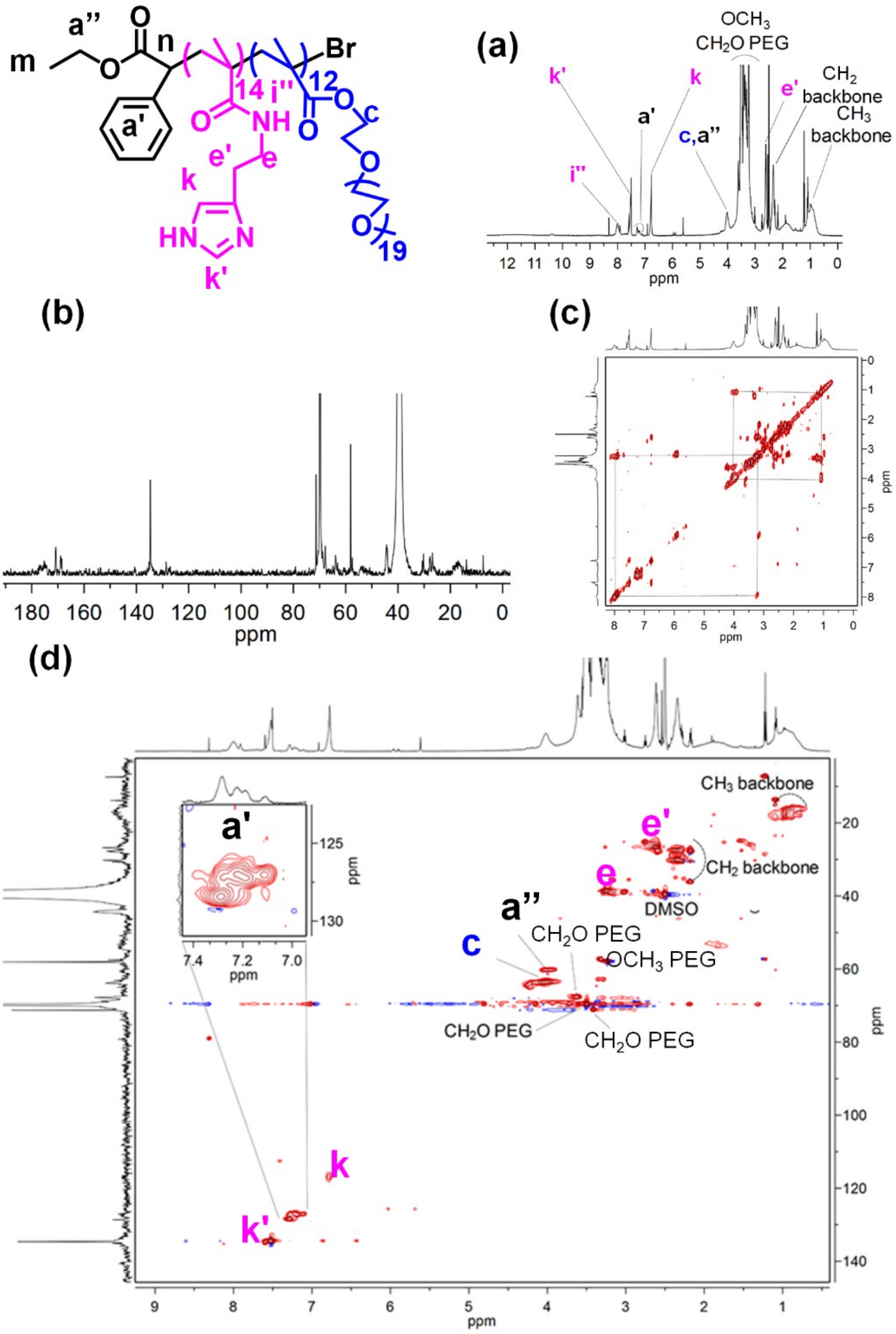

Figure S6. Quantitative ^{1}H (a) and ^{13}C $\{^1$H$\}$ inverse gated decoupled (b) NMR spectra of L2. (c) ^{1}H-^{1}H COSY and (d) ^{1}H-^{13}C HSQC of L2. All spectra were recorded in DMSO-d_6 at 25°C on a Bruker 600 MHz Cryoprobe spectrometer. All the characteristic signals of polymer ligand L2 are assigned. The integration between proton a' (5H) and c, a" (2H) enables the quantification of the total number of proton c and a" to be 24. After the subtraction of proton a" (2H), the number of proton c is 22 which corresponds to 11 PEG chains. This value is in a good agreement with the number found in the case of polymer precursor that was measured by using conventional NMR (12).

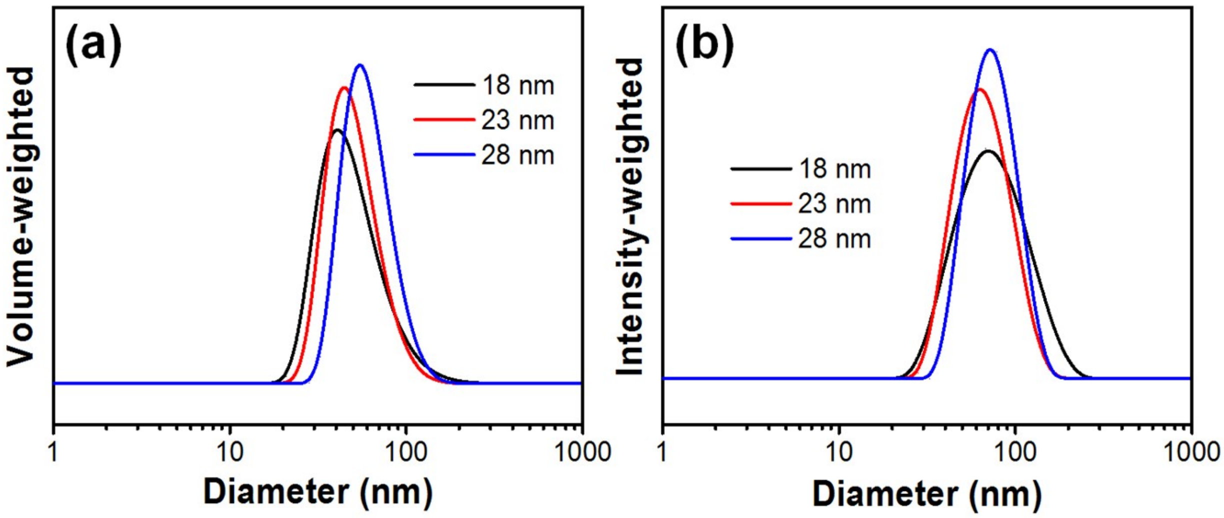

Figure S7. DLS traces of different edge length IONCs upon water transfer process weighted by (a) volume and (b) intensity.

Table S3. Zeta potential of IONCs with different size transferred in water using L1

IONCs edge (nm)	Zeta potential (mV)
18	- 20.1 ± 2.1
23	- 21.0 ± 1.3
28	- 19.2 ± 3.4

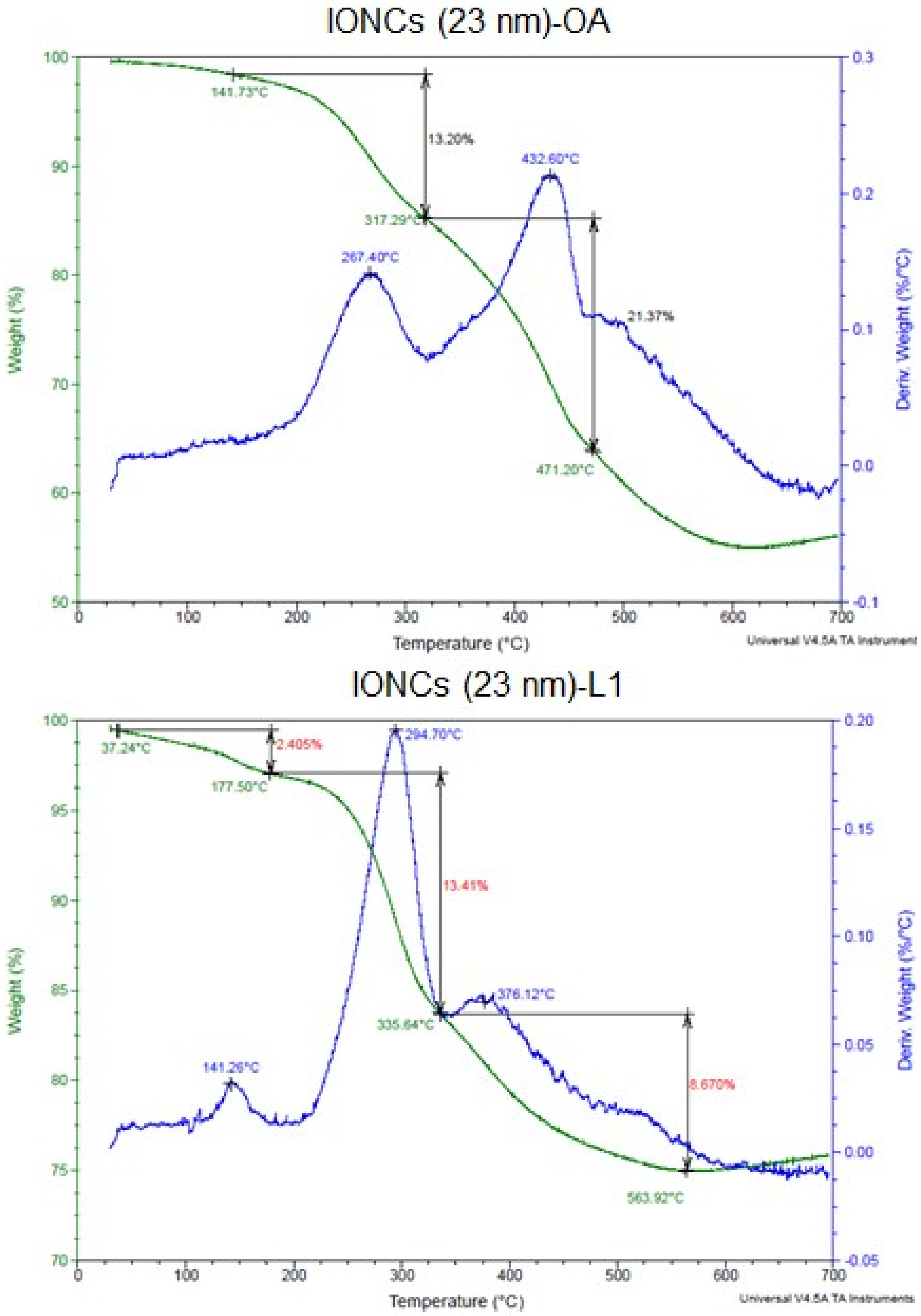

Figure S8. TGA graphs descibe the weight loss of prisitne IONCs (23 nm) and the one upon water transfer using L1 during the heating ramp.

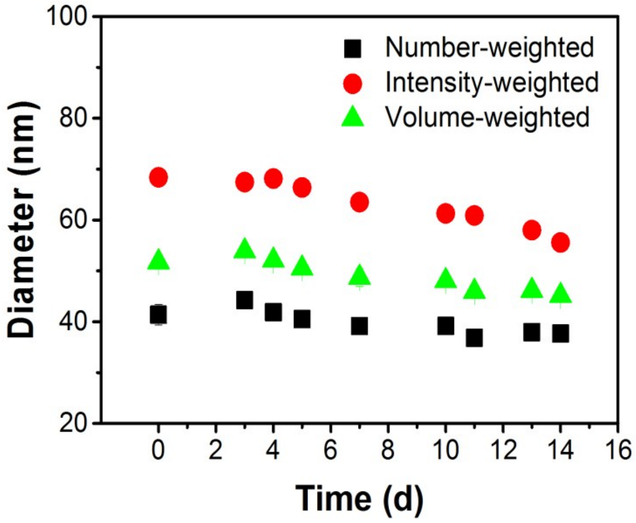

Figure S9. d_H (measured by DLS, number, intensity and volume-weighted) of IONCs (23 nm) modified with P(PEGMA$_{950}$-*co*-PAEMA-*co*-MAA) dispersed in saline upon long term storage at room temperature.

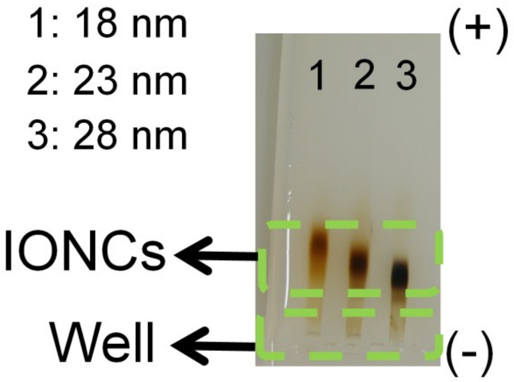

Figure S10. The migration of IONCs with different sizes transferred in water using P(PEGMA$_{950}$-*co*-PAEMA-*co*-MAA) upon 2 years of storage. The measurement was performed in agarose gel (1.0 % wt, 100 V and 60 min).

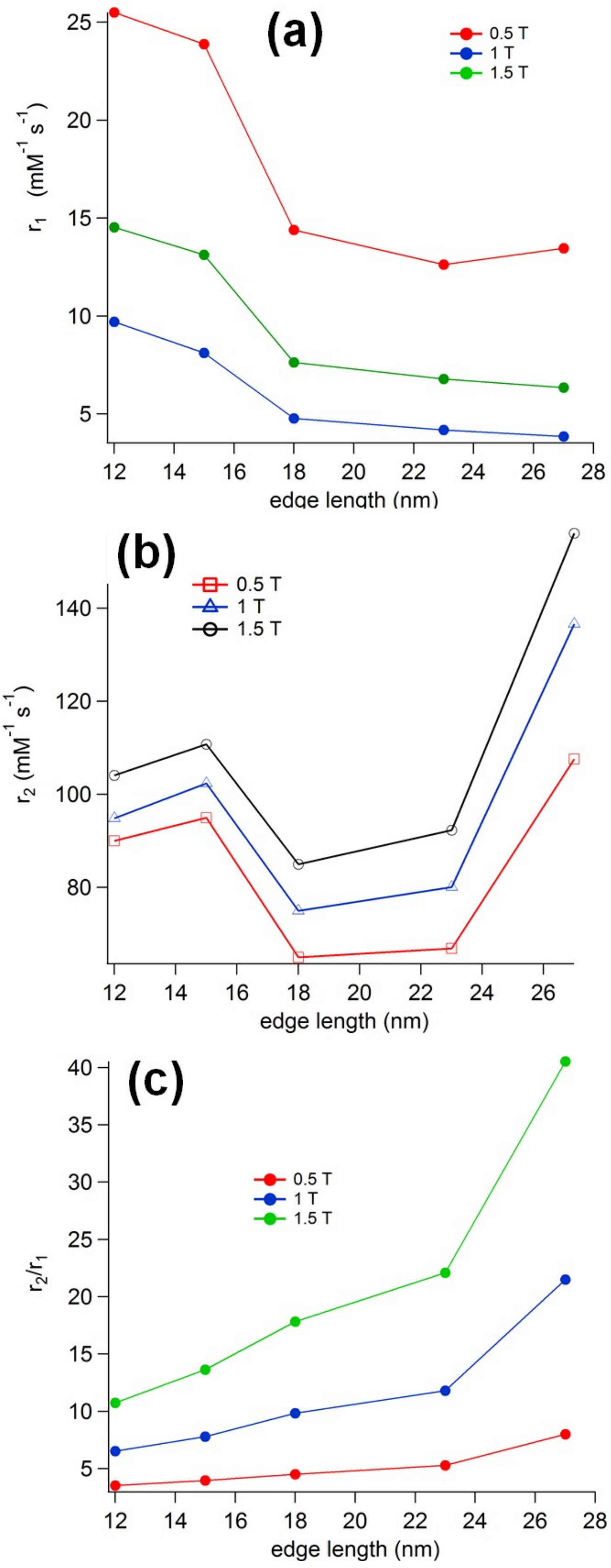
(a)
0.5 T
1 T
1.5 T
r_1 (mM^{-1} s^{-1})
25
20
15
10
5
12
14
16
18
20
22
24
26
28
edge length (nm)
(b)
0.5 T
1 T
1.5 T
r_2 (mM^{-1} s^{-1})
140
120
100
80
12
14
16
18
20
22
24
26
edge length (nm)
(c)
0.5 T
1 T
1.5 T
r_2/r_1
40
35
30
25
20
15
10
5
12
14
16
18
20
22
24
26
28
edge length (nm)

Figure S11. Relaxometry measurement of IONCs with different sizes transferred in water using L1 polymer. At different magnetic field (0.5, 1 and 1.5 T) the r2/r1 ratio (c) between the transversal (r2) (b) and longitudinal (r1) (a) relaxations suggest that these MRI agents are T2-type contrast agents.

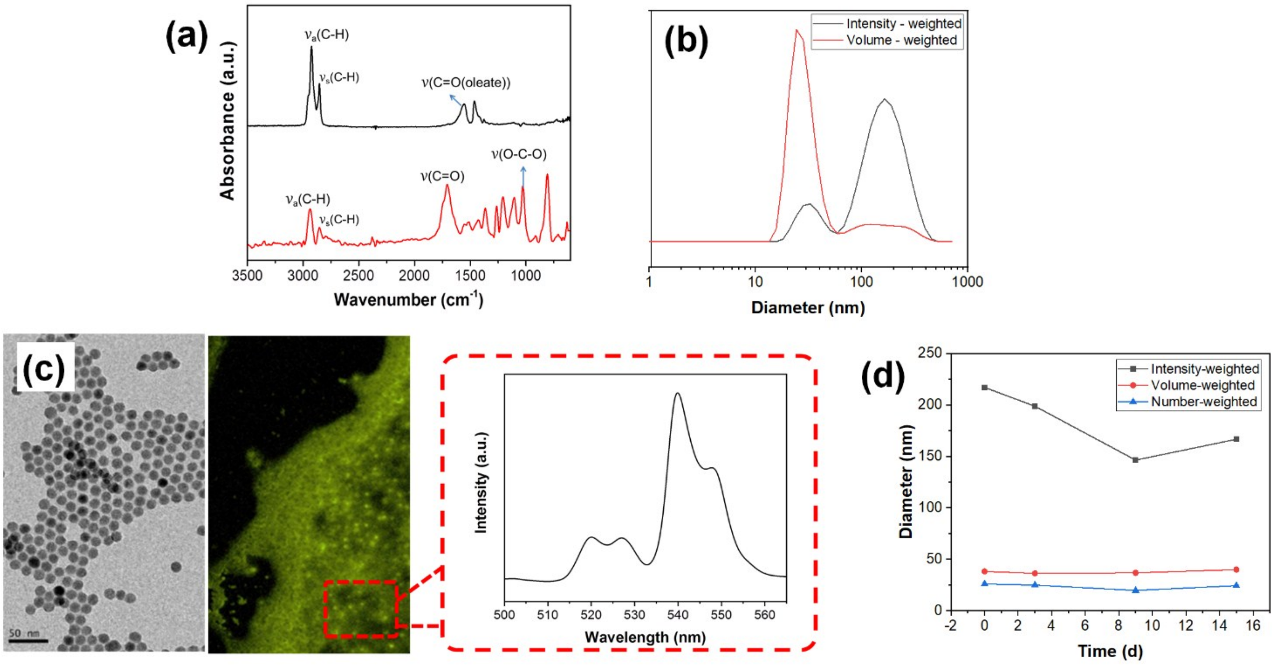

Figure S12. (a) FT-IR spectra of pristine UCNPs (black curve) and the one upon the ligand exchange and removal of unbounded ligands (red curve). (b) The DLS traces of UCNPs modified with L1 in water weighted by volume and intensity. (c) The TEM images of pristine UCNPs and the confocal images showing the fluorescence of pristine UCNPs (excited at 980 nm) and the photoluminescence spectra of pristine UCNPs at the area of interest in confocal image. (d) The d_H (measured by DLS, number, intensity and volume-weighted) of the UCNPs modified with L1, dispersed in saline solution, after being stored for a long time at room temperature.

β-NaYF$_4$:30%Gd:18%Yb:2%Er-OA

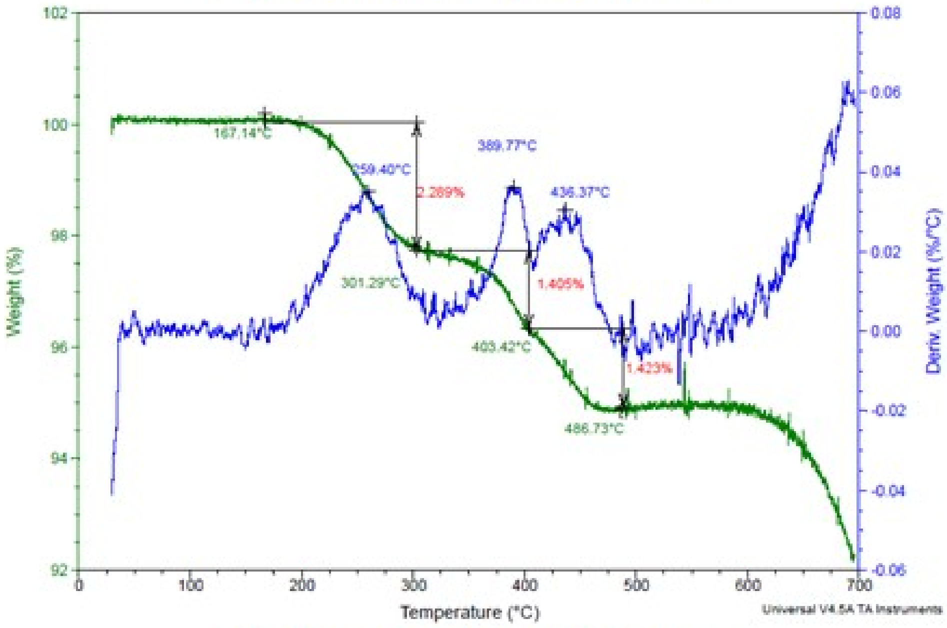

β-NaYF$_4$:30%Gd:18%Yb:2%Er-L1

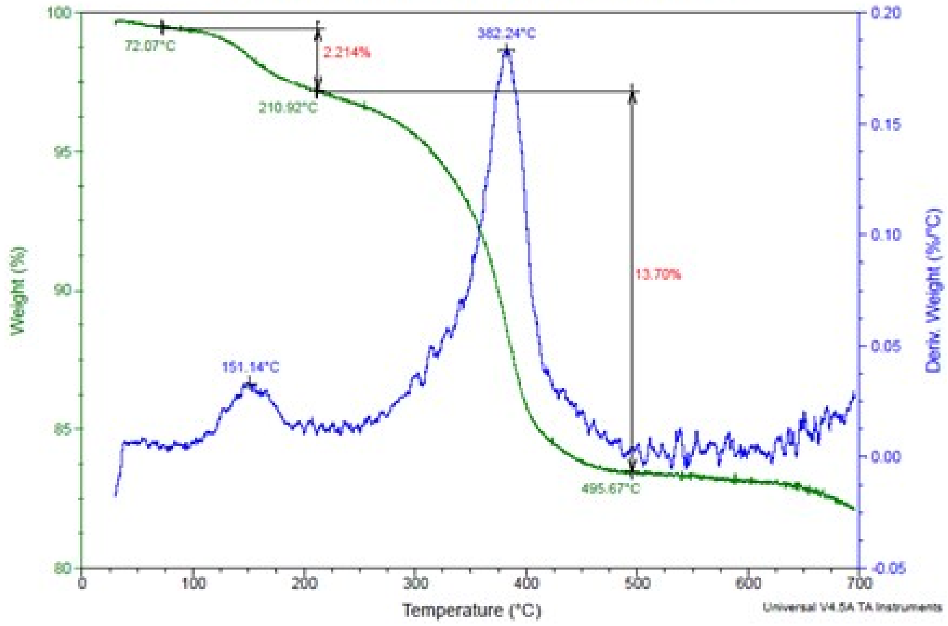

Figure S13. TGA graphs descibe the weight loss of prisitne UCNPs and the one upon water transfer using L1 during the heating ramp.

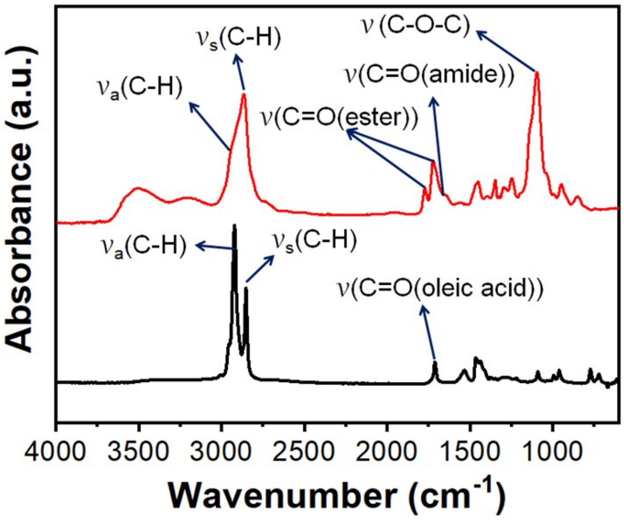

Figure S14. FT-IR spectra of pristine CdSe@CdS (black curve) and the one upon the ligand exchange and removal of unbounded ligands (red curve).

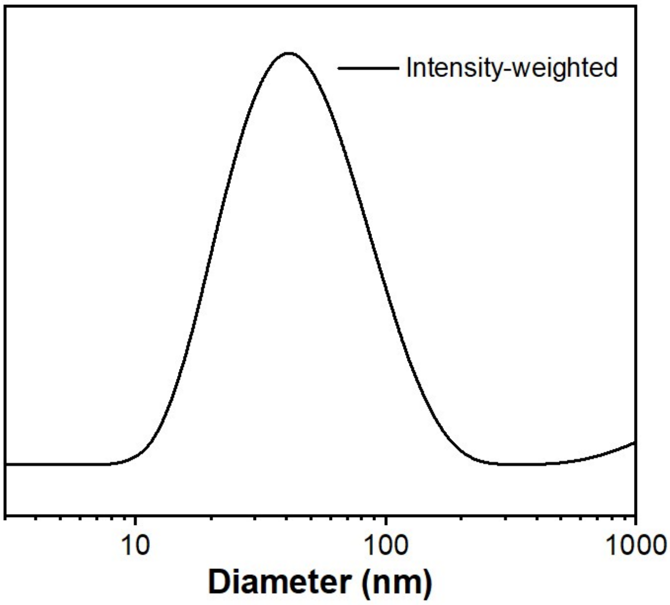

Figure S15. DLS traces of QDs upon water transfer process with L1 weighted by intensity.

CdSe@CdS-OA

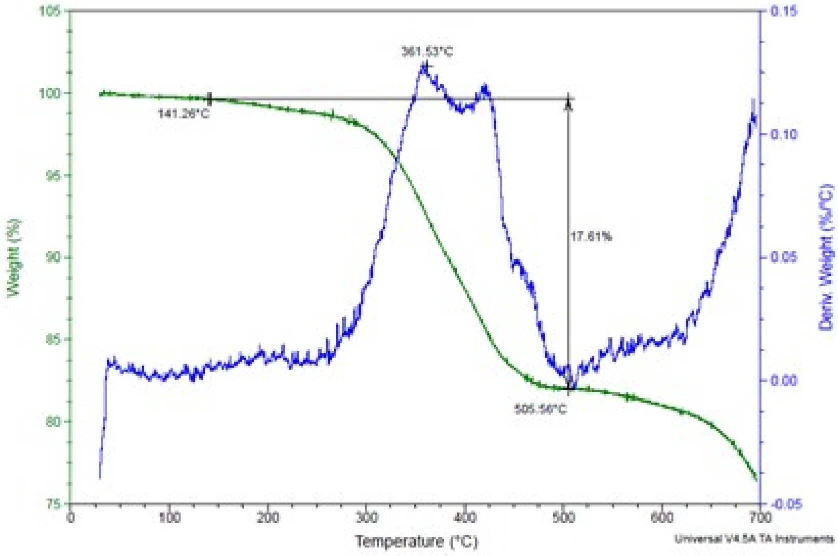

CdSe@CdS-L1

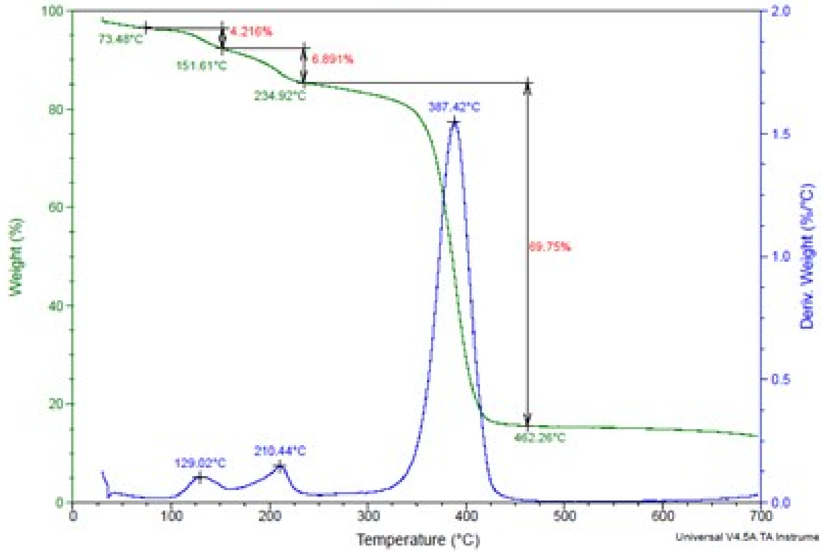

CdSe@CdS-L2

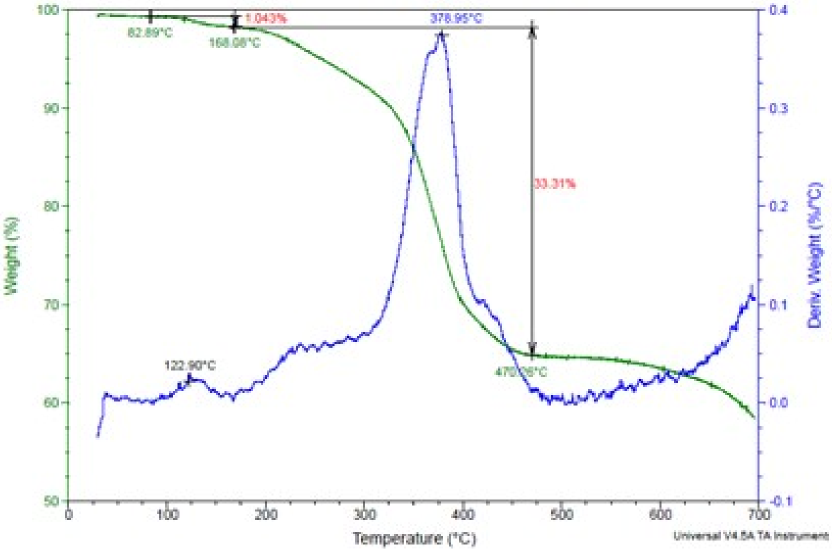

Figure S16. TGA graphs descibe the weight loss of prisitne CdSe@CdS QDs (a) and the one upon water transfer using L1 (b) and L2 (b) during the heating ramp.

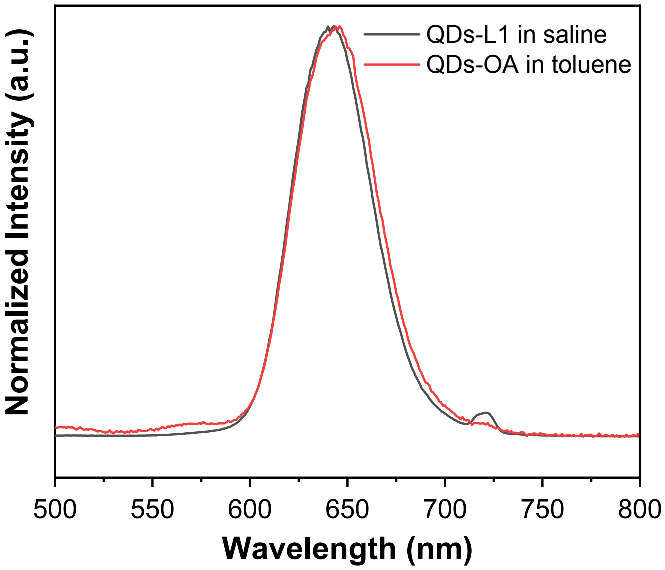

Figure S17. PhotoLuminescent spectra of original CdSe@CdS QDs in toluene and L1 modified QDs in saline (excitation wavelength 360 nm).

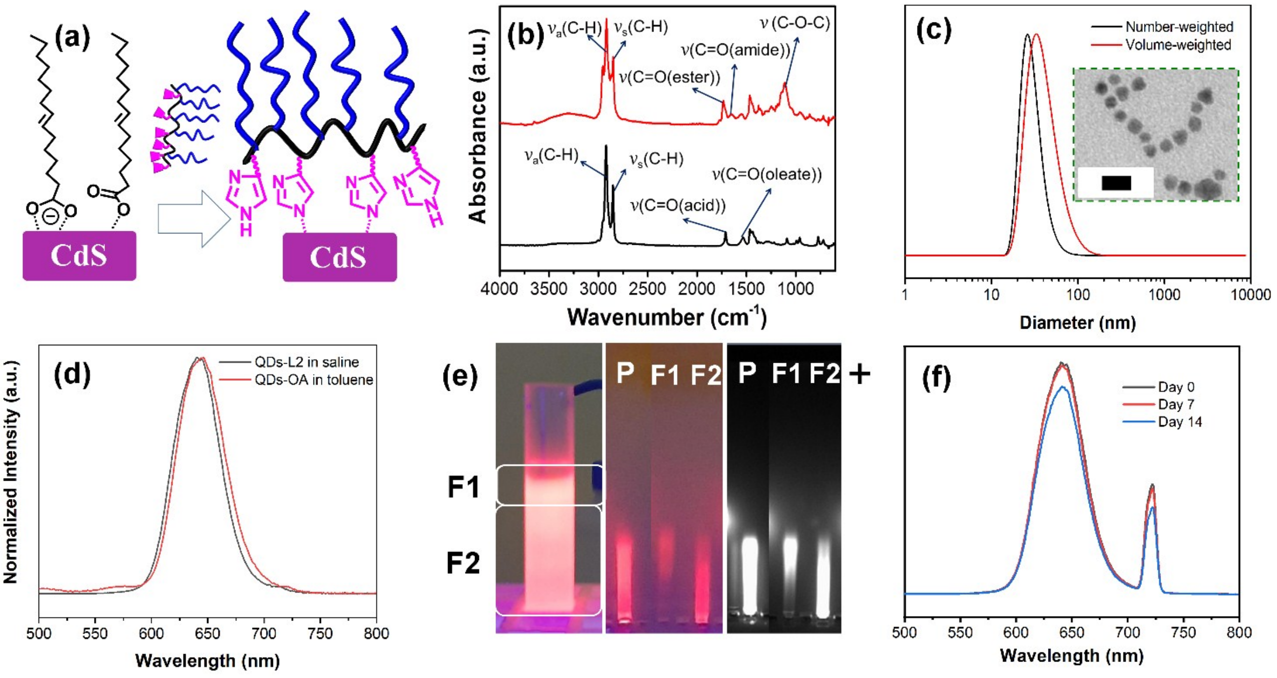

Figure S18. Water transfer of CdSe@CdS QDs using ligand P(PEGMA$_{950}$-*co*-IEMA) L2. (a) A schematic representation describes the change on QDs surface upon the ligand exchange, the ligand exchange was carried out following a same procedure described for the case of IONCs and UCNPs however the use of TEA in this case is omitted. (b) FT-IR spectra of pristine QDs (black curve) and the one upon the ligand exchange and removal of unbounded ligands (red curve). (c) DLS traces (number- and volume-weighted) of

QDs upon the water transfer process. Inset: TEM images of QDs in water. (d) PhotoLuminescent spectra of original CdSe@CdS QDs in toluene and P(PEGMA$_{950}$-*co*-IEMA) modified QDs in saline (excitation wavelength 360 nm). (e) The UV (365 nm) exposed images of the ultracentrifugation tube containing L1-functionalized QDs along sucrose gradient (60:40:20%) (15000 rpm, 45 min) (left); the migration of pristine QDs-L1 (P), low density fraction (F1) and higher density fraction (F2) that were collected from the ultracentrifugation tube in the agarose gel (1%, 100 V, 45 min) (middle). The same images of the gel recorded under UV with a wavelength cut off of 630 nm was shown in the right panel. (f) PhotoLuminescent spectra of CdSe@CdS QDs functionalized with L1 in saline at different storing time. (excitation wavelength 360 nm). Signals at 720 nm are due to the excitation. Saline was used in all characterizations.

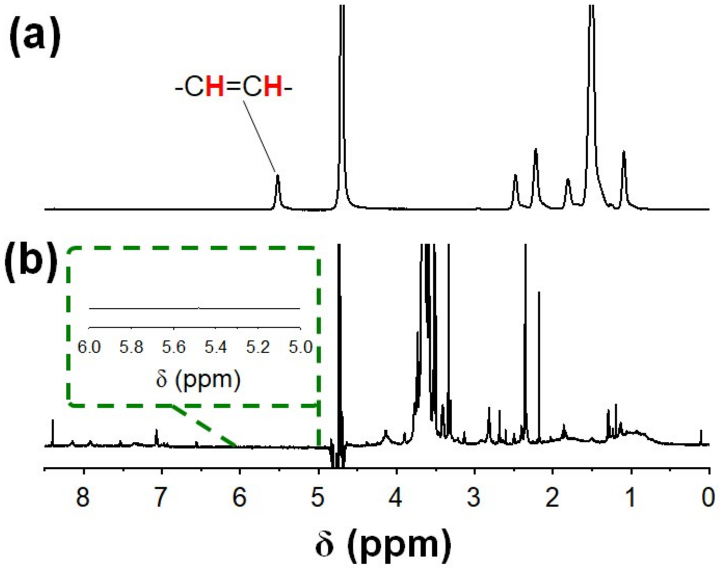

Figure S19. ^1H NMR spectrum of oleic acid in D_2O (a) and 1D noesy presat ^1H spectrum of CdSe@CdS-L2 in H_2O/D_2O (15% D_2O) (b) recorded on a Bruker 600 MHz Cryoprobe spectrometer at 25°C.

Quantum yield of CdSe@CdS coated P(PEGMA$_{950}$-*co*-IEMA)

Quantum Yield of QDs was measured by comparison with a dye of known quantum yield. The dye chosen for the measurement was cresyl violet. The dye has an emission in the range of our QDs (Figure S20) with a QY=0.54 in methanol.[1] Another important characteristic is the fact that this dye is not quenched by the oxygen dissolved in the solvents, thus allowing us to work with air-equilibrated methanol.

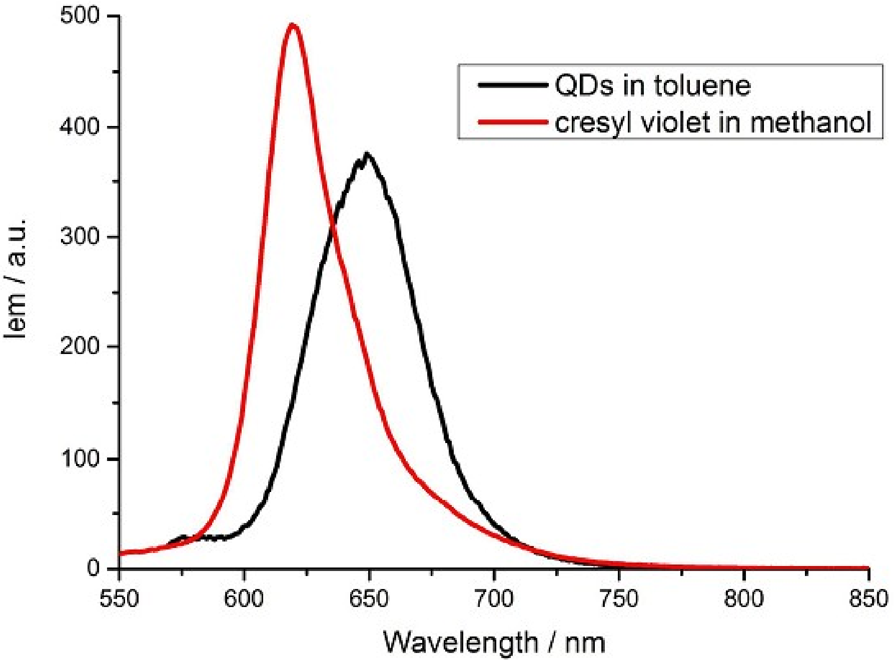

Figure S20. Emission spectra of a solution of cresyl violet in methanol and QDs in toluene excited at 360 nm

Spectra were recording exciting at a wavelength in which both solutions have the same absorbance. In this conditions and taking into account that absorbance at the excitation wavelength and in the range of the emission is below 0.1, the general formula can be reduced as reported in eq 1

$$\Phi = \Phi_r \times \frac{I}{I_r} \times \frac{n^2}{n_r^2}$$

Equation 1

where φ_r is the quantum yield of the reference dye, I is the integration of the emission spectra of the QDs, I_r is the integration of the emission spectra of the reference, n is the refractive index of the QD's solvent and n_r is the refractive index of the reference dye's solvent.

QY of the pristine sample was calculated following equation 1 and taking into account that I QDs was 21313, I reference was 23453, QY cresyl violet was 0.54, refractive index of MeOH was 1.3314 and refractive index of toluene was 1.4969. QY of toluene soluble QDs was 0.61.

Table S4. Luminescence quantum yield data

n MeOH	1.3314	QY Cresyl Violet in MeOH	0.64
n Toluene	1.4969		

λ excitation (nm)	IIntensity in Toluene **QDs**	IIntensity in MeOH **Cresyl Violet**	Relative QY
600 nm	21313.3	23453.4	**0.61**

QY of water soluble QDs, was calculated using the pristine QDs as reference. A solution of water soluble and toluene soluble QDs were first prepared (Figure S21).

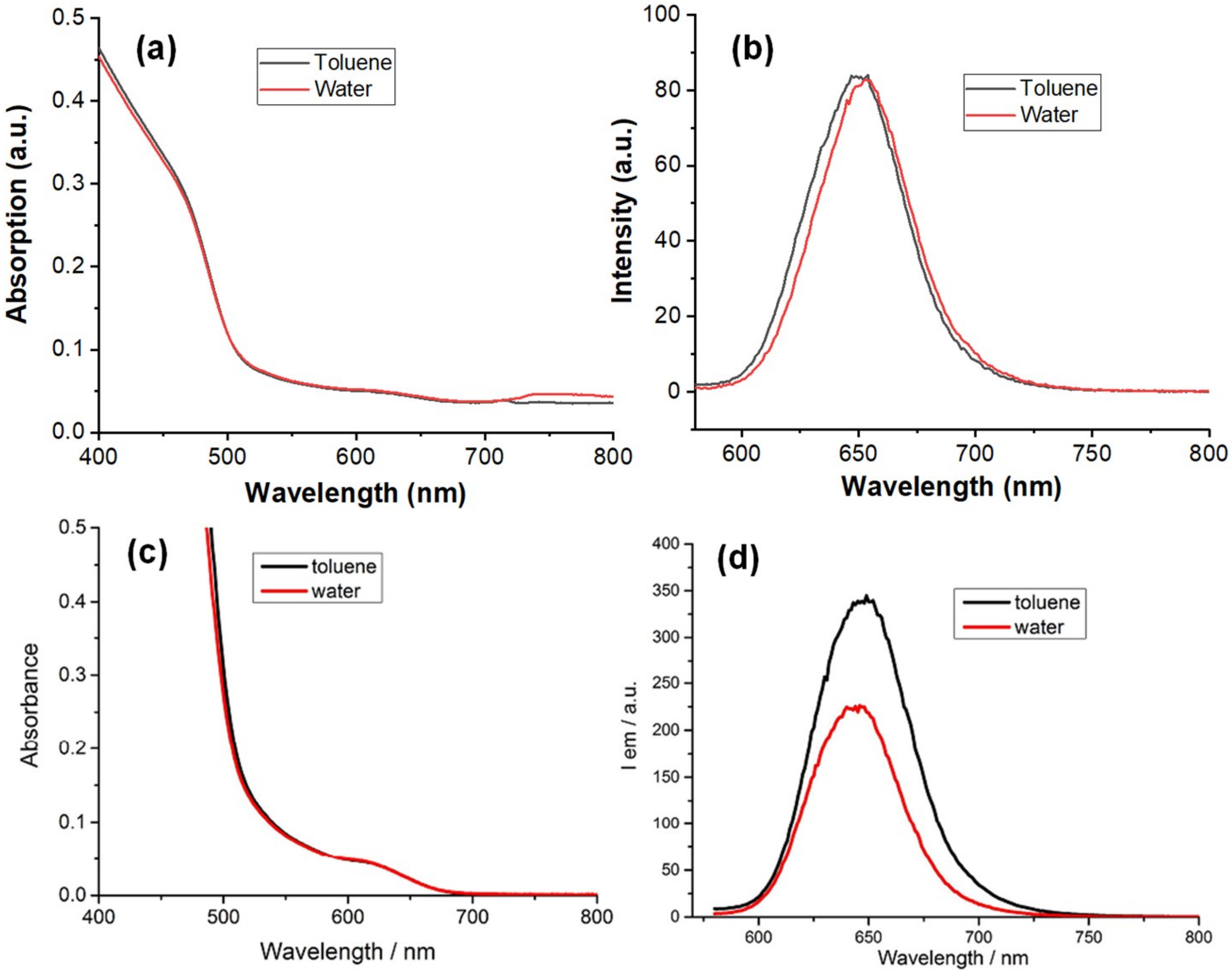

Figure S21. Absorption and emission spectra (excited at 360 nm) of CdSe@CdS-L2 (a, b) and CdSe@CdS-L1 (c, d, excited at 570 nm) in toluene and water.

Then three different spectra were recorderd for both type of QDs and calculation were made based on the equation1, taking into account that QY of QDs soluble in toluene was 0.61, n toluene 1.4969 and n water 1.33. Results are gathered in Table S5 and S6. Average QY of water soluble QDs capped with L1 and L2 was 0.48 and 0.31, respectively.

Table S5: Luminescence quantum yield data for CdSe@CdS-L1 in water.

n Toluene	1.4969	QY CdSe@CdS in toluene	0.61
n Water	1.33		
λ excitation (nm)	**I**Intensity in water **QDs**	**I**Intensity in toluene **QDs**	Relative QY
570 nm	4331.4	4616.0	0.47
590 nm	3652.1	3790.2	0.49
620 nm	3437.3	3633.5	0.48
			0.48

Table S6: Luminescence quantum yield data for CdSe@CdS-L2 in water.

n Toluene	1.4969	QY CdSe@CdS in toluene	0.61
n Water	1.33		
λ excitation (nm)	**I**Intensity in water **QDs**	**I**Intensity in toluene **QDs**	Relative QY
570 nm	11848.5	18983.3	0.32
590 nm	12860.4	20733.5	0.31
620 nm	12784.6	21010.7	0.31
			0.31

1. Montalti, M.; Credi, A.; Prodi, L.; Gandolfi, M. T., *Handbook of photochemistry*. CRC press: 2006.